Synthesis and Characterization of Poly(acrylic acid) Stabilized Cadmium Sulfide Quantum Dots

Serdar Celebi,[†] A. Koray Erdamar,[‡] Alphan Sennaroglu,[‡] Adnan Kurt,[‡] and Havva Yagci Acar*[,§]

Graduate School of Materials Science and Engineering, Laser Research Laboratory, Department of Physics, and Department of Chemistry, Koc University, Rumelifeneri Yolu, Sariyer 34450, Istanbul, Turkey

Received: May 22, 2007; In Final Form: September 4, 2007

Cadmium sulfide (CdS) nanoparticles (NPs) capped with poly(acrylic acid) (PAA) were prepared in aqueous solutions from $Cd(NO_3)_2$ and Na_2S. Influence of the COOH/Cd ratio (0.8−12.5), reaction pH (5.5 and 7.5), and PAA molecular weight (2100 and 5100 g/mol) on the particle size, colloidal stability, and photoluminescence were investigated. A Cd/S ratio of <1 causes ineffective passivization of the surface with the carboxylate and therefore results in a red shift of the absorption band and a significant drop in photoluminescence. Therefore, the Cd/S ratio was fixed at 1.1 for all experiments studying the mentioned variables. PAA coating provided excellent colloidal stability at a COOH/Cd ratio above 1. Absorption edges of PAA-coated CdS NPs are in the range of 460−508 nm. The size of the NPs increases slightly with increasing PAA molecular weight and COOH/Cd ratio at pH 7.5. It is demonstrated that there is a critical COOH/Cd ratio (1.5−2) that maximizes the photoluminescence intensity and quantum yield (QY, 17%). Above this critical ratio, which corresponds to smaller crystal sizes (3.7−4.1 nm) for each reaction set, the quantum yield decreases and the crystal size increases. Moreover, CdS NPs prepared at pH 7.5 have significantly higher QY and absorb at lower wavelengths in comparison with those prepared at pH 5.5. Luminescence quenching has not been observed over 8 months.

Introduction

Semiconductor quantum dots (QD) have been the subject of extensive research due to their unique size-dependent optical properties and widespread applications in science and technology. Quantum confinement of excitons at crystal sizes comparable to or below the exciton Bohr radius creates size-tunable narrow bandwidth photoluminescence.[1] As the size of the semiconductor crystal decreases, the band gap between the conduction and the valence bands increases.[2] This results in a size-dependent absorption onset and emission wavelength, both becoming blue-shifted with decreasing particle size.[3] Therefore, the color output can be tuned by varying the size and the nature of the QD. Group II−VI semiconductor nanocrystals, such as CdS, CdSe, and CdTe, have been studied widely as they emit in the visible region.[4,5] There is a tremendous effort to improve and control QDs which enable innovations in a broad spectrum of areas including solar cells, light emitting diodes (LEDs), sensors, lasers, medical imaging, and biological labeling.[6−10] Long-term photostability, high quantum yield (QY), and narrow spectral bandwidth make QDs excellent fluorescent tags with better sensitivity compared to organic fluorescent molecules. The possibility to excite various size QDs simultaneously with a single excitation wavelength provides opportunity for color multiplexing which is revolutionary in barcoding and labeling.[6,11]

Since the unique properties of QDs are based on size, controlling size and size distribution as well as crystallinity and surface defects is crucial. Nanoparticles (NPs) are usually prepared as core−shell structures, in which an organic shell is adsorbed on the crystal surface to control the particle growth through surface passivization (arrested).[12] The organic shell is also responsible for the dispersion of particles in a carrier solvent, prevention of aggregation, and colloidal stability. Effective surface passivization is also crucial for optical properties such as photobleaching and quantum efficiency. Surface defects usually cause radiationless recombination of the excitons which limits luminescence efficiency.[13]

The best quality QDs are generally provided by high-temperature synthesis using the stringent Schlenk techniques from toxic organometallic precursors with hydrophobic coatings such as tri-octyl phospine oxide (TOPO).[14] However, for many biological applications, the transfer of QDs to water is necessary. Ligand exchange of TOPO with water-soluble molecules and bilayer formation are proven methods to provide aqueous suspensions of QDs.[15−17] However, they usually suffer from drawbacks such as dramatic reduction in the quantum efficiency, colloidal stability, or an increase in the overall hydrodynamic size. Therefore, preparation of particles directly in aqueous solutions is a very practical approach and, usually, a milder, greener synthetic route. Yet, it is a challenge to prepare QDs in desired sizes and narrow size-distribution with high quantum efficiency and colloidal stability with the aqueous synthetic routes. Molecules with thiol (−SH) groups are proven to be effective coatings for CdS and CdSe. In aqueous systems, bifunctional molecules are desired where the thiols adsorb on the crystal surface and the other functional groups provide a favorable interaction with the solvent to suspend particles. Few examples are thioacetamide,[18] cystein,[19] mercaptoethanol,[20] mercaptopropionic acid,[20,21] and mercaptopropyl trimethoxysilane.[22] Korgel et al. reported a detailed study on mercaptoacetic

[†] Graduate School of Materials Science and Engineering.
[‡] Laser Research Laboratory, Department of Physics.
[§] Department of Chemistry.

10.1021/jp0739420 CCC: $37.00
Published on Web 10/12/2007

acid (MAA)-coated CdS QDs prepared in water and discussed the influence of pH and coating amount on the size and luminescence.[23] In MAA-CdS, thiolates bind competitively to the surface cations. Although quantum efficiencies were not reported, maximum photoluminescence (PL) intensity was reported to be achieved at a pH range of 6−8 at the MAA/Cd ratio of 11−20. The ligand concentration does not have a significant effect on the absorption wavelength or the PL peak position of the MAA-CdS particles. However, both of these have a red shift with increasing pH of the solution before Na_2S addition. Such behavior was attributed to HS^- mediated crystal growth and the thiol complexes formed between the ligand and Cd^{2+} ions. They also suggest that many times the changes in the size and luminescence is not due to the ligand concentration but to the related change in pH.

We are interested in the preparation of PAA-coated CdS in a low-temperature aqueous process. Polymeric coatings are effective on providing steric stabilization for colloidal nanoparticles. PAA, a polyelectrolyte, would also provide electrostatic stabilization. In addition, each polymer chain provides multiple adsorption sites, and the coated particles would have free carboxylate groups available for further functionalization.

There are few reports on the templated synthesis of CdS in PS-b-PAA block-copolymer micelles with a focus on the ionic core size and the aggregation number. These particles had a hydrophobic PS shell, and all QDs were prepared in the PAA core.[24,25] Eisenberg expanded this system to PEO-b-PS-b-PAA triblock polymers to create different morphologies such as multicore and worm-like micelles.[26] Zhang, reported an example of PAA(1000 g/mol)-coated CdS nanoparticles to prepare polyaniline wires through complex formation but does not focus on the PAA-CdS system itself or its optical properties.[27]

To the best of our knowledge, this is the first report in the literature investigating the influence of PAA molecular weight and amount on particle properties such as crystal size, photoluminescence emission intensity, QY, and colloidal stability of aqueous CdS-PAA QDs. PAA with 2100 and 5100 g/mol molecular weights were used as coatings. We also investigated the influence of reaction pH on the size and optical properties. CdS QDs were prepared at a pH of 7.5 with varying amounts of PAA at both molecular weights. In a different set of reactions, QDs were prepared at pH 5.5 using PAA 2100 g/mol. The effect of the Cd/S ratio on particle properties was also studied. Influence of the variables on size and optical properties was determined through absorption (UV−vis range) and photoluminescence analysis.

Experimental Section

Materials. All chemicals were analytical grade or of the highest purity available. Sodium sulfide trihydrate ($Na_2S{\cdot}3H_2O$), mercaptoacetic acid ($HSCH_2COOH$), cadmium nitrate tetrahydrate ($Cd(NO_3)_2{\cdot}4H_2O$), Rhodamine B, and HNO_3 (65%) were purchased from Merck. Sodium hydroxide and PAA sodium salts (PAA2K: 2100 g/mol and PAA5K: 5000 g/mol) were purchased from Aldrich. Only double-distilled Milli-Q water (Millipore) was used as the solvent.

Synthesis of CdS Stabilized with PAA. In a typical synthesis, 64.3 mg of $Cd(NO_3)_2{\cdot}4H_2O$ was dissolved in 100 mL of water and transferred into a 500 mL, three-necked round-bottomed flask fitted with a mechanical stirrer. An appropriate amount of PAA (MW = 2100 g/mol) was dissolved in 150 mL of water, added to Cd solution, and deoxygenated with nitrogen for 10 min. For reactions run at pH 7.5, pH was adjusted with 10 M NaOH and/or 10 M HNO_3. Sulfide solution was prepared by dissolving 25 mg of $Na_2S{\cdot}3H_2O$ in 50 mL of water and injected into the reaction mixture. The reaction mixture was kept stirring at room temperature under nitrogen for an hour. pH usually increases by 0.5−1.0 units after Na_2S addition, and the reaction ends around pH 8.0−8.5. No further pH adjustment was done before UV−vis or PL measurements. An appropriate amount of PAA was calculated based on the desired COOH/Cd ratio. All ratios are listed in Table 1.

TABLE 1: Average Size and Band Gap of CdS NPs Calculated from UV−Vis Spectra

sample ID[a]	COOH/Cd	Cd/S	abs. cutoff (λ)	size[b] (nm)	band gap[c] (eV)	fwhm[d] (nm)
PAA 2K-1a	1.0	1.1	460	3.6	2.70	181.5
PAA 2K-2a	1.6	1.1	464	3.7	2.68	161.0
PAA 2K-3a	2.1	1.1	486	4.5	2.55	176.5
PAA 2K-4a	2.5	1.1	488	4.6	2.54	179.5
PAA 2K-5a	3.3	1.1	492	4.9	2.52	177.0
PAA 2K-6a	11.2	1.1	459	3.6	2.71	153.0
PAA 2K-1b	0.8	1.1	490	4.8	2.53	189.5
PAA 2K-2b	1.5	1.1	487	4.6	2.55	163.5
PAA 2K-3b	2.0	1.1	477	4.1	2.60	165.5
PAA 2K-4b	3.0	1.1	477	4.1	2.60	182.5
PAA 2K-5b	5.0	1.1	484	4.4	2.57	193.5
PAA 2K-6b	8.1	1.1	488	4.6	2.54	173.0
PAA 2K-7b	11.2	1.1	490	4.8	2.53	196.5
PAA 2K-8b	13.1	1.1	489	4.7	2.54	201.5
PAA 5K-1a	1.6	1.1	463	3.7	2.68	161.0
PAA 5K-2a	2.5	1.1	476	4.1	2.61	160.5
PAA 5K-3a	5.0	1.1	508	6.5	2.44	143.0
PAA 5K-4a	12.5	1.1	506	6.2	2.45	133.5
PAA 5K-5a	1.6	2.5	470	3.9	2.64	164.5
PAA 5K-6a	1.6	0.6	490	4.8	2.53	152.5

[a] Samples labeled with 'a' are synthesized at pH 7.5 and 'b' at pH 5.5. [b] Calculated by Brus effective mass approximation.[2] [c] Corresponding band gap energy calculated by $E = h\nu$. [d] Full-width at half-maximum calculated from PL spectra.

Instrumentation. FTIR spectra were recorded on a Jasco FT-IR-600 spectrometer. Absorption spectra were recorded with a UV−vis−NIR spectrophotometer (Schimadzu, model 3101 PC) in the 300−600 nm range. Absorption of samples at the excitation wavelength was kept around 15% by diluting the samples with water. The size of the CdS NPs was calculated by using the Brus equation:[2]

$$\Delta E = \left(\frac{\hbar^2\pi^2}{2R^2}\right)\left(\frac{1}{m_e} + \frac{1}{m_h}\right) - 1.8\frac{e^2}{\epsilon_{CdS}R} \qquad (1)$$

Here, ΔE is the band gap shift, R is the corresponding shell radius of CdS NPs, m_e and m_h are the effective mass of electrons and holes, and ϵ_{CdS} is the relative dielectric constant of the bulk CdS. In our calculations, the bulk band gap of CdS was taken as 2.41 eV.[28]

For evaluation of photoluminescence and calculation of quantum efficiencies, samples were excited at a wavelength of 355 nm. The experimental setup used in the luminescence measurements is shown in Figure 1. A pulsed, 1064 nm Nd:YAG laser operating at a repetition rate of 1 kHz and outputting 140 ns pulses was used to generate the ultraviolet pump at 355 nm. The 1064 nm output was first frequency doubled in a 10 mm long potassium titanyl phosphate crystal (KTP) to 532 nm. The fundamental (1064 nm) and the second harmonic (532 nm) were then mixed inside a 20 mm long lithium triborate (LBO) crystal to obtain sum-frequency generation at 355 nm. In the experiments, 355 nm pulses with energies of up to 13 μJ were available. In the luminescence measurements, the 355 nm pump beam was focused inside the aqueous QD solutions. The emitted

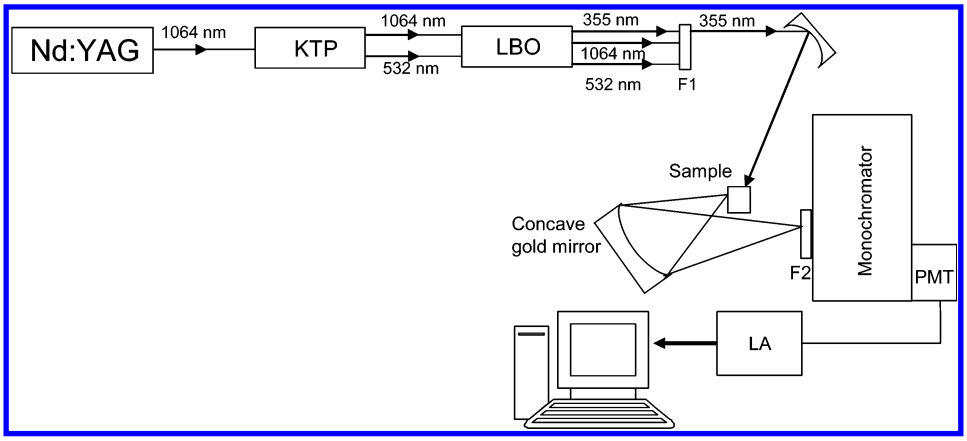

Figure 1. Schematic of the luminescence measurement setup.

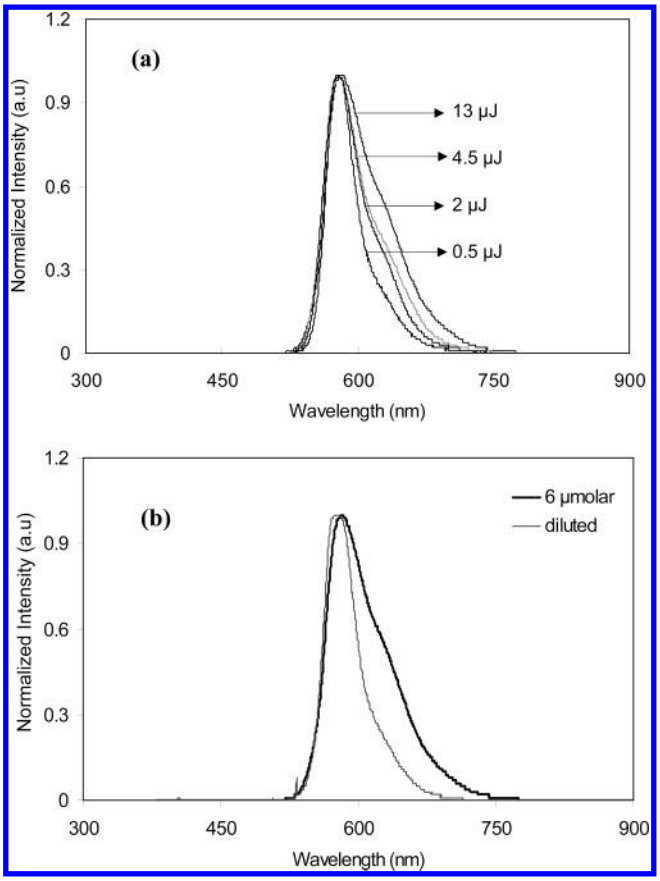

Figure 2. (a) Normalized PL spectra of Rhodamine B (6 μM) at different pump energies. (b) Normalized PL spectra of Rhodamine B at different concentrations (pump energy = 13 μJ); diluted Rhodamine B has 2.82% absorption at 355 nm.

fluorescence was then collected with a concave gold mirror and imaged to the entrance slit of a 0.5 m, Czerny-Turner type monochromator (CVI, model DK 480). A long pass filter was used in front of the slit to cut light below 380 nm. The luminescence signal was detected with a photomultiplier tube (PMT) and amplified with a lock-in amplifier. In order to compare the luminescence efficiencies of the samples, the emission spectra were calibrated with respect to absorbed pulse energy at 355 nm.

In order to estimate the absolute luminescence QY of the samples, the calibrated emission spectra of the samples were compared with that of 6 μM Rhodamine B solution. The total integrated luminescence intensity Σ_I of each sample was first determined by calculating the area under the luminescence band. The relative luminescence QY (η) was then calculated from

$$\eta = \frac{\Sigma_I}{\Sigma_{RhB}} \quad (2)$$

where Σ_{RhB} is the integrated luminescence intensity for Rhodamine B for the same absorbed pump power.[29]

Since pulse laser excitation was used in the QY measurements, care was taken to minimize intensity- and concentration-dependent spectral broadening of the Rhodamine B emission band, and optimum pump energy and Rhodamine B concentration were experimentally selected for dependable comparison. Figure 2 shows the normalized emission spectra of Rhodamine B at different pumping levels (concentration = 6 μM) and at different concentrations (pumping energy = 13 μJ), respectively. Note that as the pumping energy or concentration is increased, the emission spectrum becomes broader possibly due to amplified spontaneous emission (ASE). At low concentrations and pumping levels, identical spectra could be obtained. In our experiments, the pump energy was kept at 13 μJ, and the diluted Rhodamine B with absorption of 2.82% at 355 nm was used. It is also important to note here that the peaks at 404 and 532 nm were ignored in the determination of the QY.

The XPS measurements were performed on a VG Ionex system equipped with a Clam II analyzer and a monochromatic Al K_α X-ray source ($h\nu$ =1486.6 eV) at the Eindhoven University of Technology. The photoelectron takeoff angle was 90° with respect to the sample surface. Sampling depth is in the range of 10 nm, depending on the kinetic energy of the ejected electrons. Excess coating was removed by dialysis before the analysis. X-ray diffraction analysis was performed by using HUBER G670 diffractometer with a germanium monochromator and Cu K_α radiation (λ = 1.5406 Å). Data collection was done in the range of $5° < 2\theta < 100°$ with 0.005° increments. Data were analyzed by using STOE WinXPOW software. Excess coating was removed by the precipitation of QDs in isopropanol before the XRD measurements.

Results and Discussions

Synthesis and Characterization of CdS-PAA. CdS nanocrystals coated with PAA have been successfully prepared at room temperature in water from nontoxic precursors. The PAA/Cd^{2+} ratio was varied at each formulation based on the mole ratio of carboxylic acid to Cd^{2+} (reported as COOH/Cd for simplicity) since two different molecular weights (2100 and 5100 g/mol) of PAA were studied. Carboxylates can chemically adsorb on the crystal and passivate the surface,

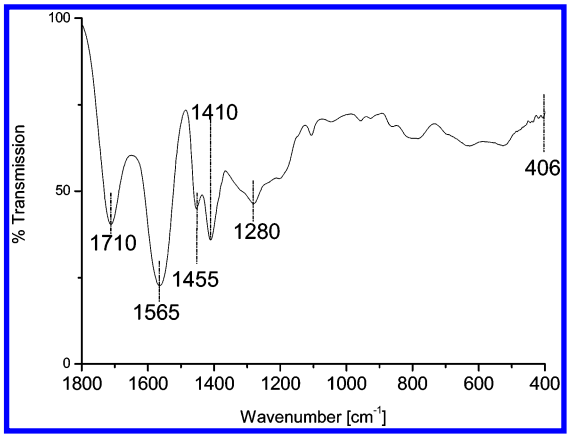

Figure 3. IR spectrum of PAA2K-coated CdS (PAA2K-6a).

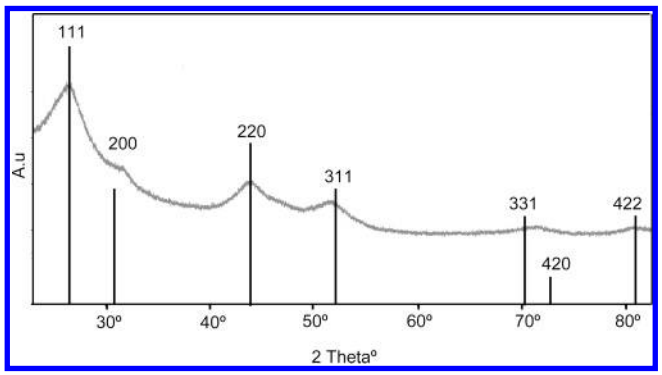

Figure 4. X-ray diffractogram of PAA 2K-2b.

controlling crystal growth and minimizing the surface defects.[24,25] Unbound carboxylate groups provide electrostatic stabilization to the aqueous CdS colloidal system. CdS with a COOH/Cd ratio of 0.8 precipitated right after the reaction, and ratio of 1 started to flocculate after 10 days. All other samples showed excellent colloidal stability over a period of more than 8 months so far.

FTIR spectrum of the PAA-coated CdS NPs (Figure 3) shows a characteristic C═O stretching peak for carboxylic acid at 1710 cm^{-1}. Peaks at 1565 and 1410 cm^{-1} correspond to asymmetric and symmetric stretching modes of carboxylate (COO^-) which are generally used to determine the binding mode of carboxylates to a surface or to a cation. A monodentate binding (from one oxygen) is usually associated with the existence of both symmetric and asymmetric stretching modes.[30] However, since only a part of the functional groups adsorbs on the CdS, it would not be possible to provide a full interpretation here. Peaks at 1455 and 1280 cm^{-1} are CH_2 bending and wagging modes of PAA backbone. The very weak peak observed around 406 cm^{-1} was attributed to the Cd−S bond.[27]

XRD analysis of CdS (PAA 2100 g/mol) shows broad peaks that are normal for nanocrystals. Two θ peaks at 26.5°, 30.7°, 44.0°, 52.1°, 70.5°, 72.6°, and 80.8° are consistent with the cubic crystal structure (a = 5.82 nm) of CdS (Figure 4). Calculated size according to the Debye−Scherrer formula[31] is 3.8 nm which is little lower than the size calculated from the UV−vis spectrum (4.6 nm) (Table 1). Broad peaks at such small sizes make size calculations difficult.

XPS analysis provided information about the existence of Cd, S, C, and O elements constituting the CdS core and the coating adsorbed on its surface (Figure 5a). Peaks at 405.6 and 162.2 eV correspond to the binding energies (BEs) of Cd $3d_{5/2}$ and S $2p_{3/2}$ consistent with the reported values for CdS (Figure 5b,c).[32] Integration of the peak areas after background subtraction and correction for atomic sensitivity factors provides information about the relative amounts of the elements. A calculated Cd/S ratio of 0.997 is consistent with the theoretical ratio of 1. There are two overlapping O 1s peaks at 532.4 and 535.4 eV, usually assigned to the carbonyl and the hydroxyl oxygen of the carboxylic acids, respectively (Figure 5d).[33] The ratio of the two is 0.994, close to theoretical ratio of 1:1. The two overlapping peaks for C 1s at 285.4−288.3 eV are in agreement with the reported binding energies for the aliphatic (backbone CH_2) and the COOH carbon, respectively (Figure 5e).[34] Ratio of the low and the high BE peaks of C 1s is 2.33, a little over the theoretical 2:1 ratio for PAA. The slightly higher amount of C might be due to the atmospheric contaminants. This also results in a C/O ratio of 2.1 which is also slightly higher than the theoretical value of 1.5.

In the UV−vis absorption spectra of the NPs (Figure 6), a blue shift (shorter wavelength) of the absorption onset was observed in comparison with bulk (2.41 eV) as a result of quantum confinement.[35] The sizes of the CdS nanocrystals were determined from the absorption onset wavelengths by using the Brus equation (see eq 1) based on the effective-mass approximation (Table 1). The absence of strong excitonic peaks on the absorbance spectra was attributed to the strong Coulomb screening and/or broad size distributions of the NPs.[36,37] All samples emit around yellow-orange when excited with UV lamp at 365 nm, but they differ in the color intensity. In order to compare the luminescence efficiencies of the samples, the emission spectra were calibrated with respect to absorption at 355 nm, where samples were excited. Calibrated emission spectra are shown in Figure 7. Note that the sharp peak is due to the stray 532 nm light that could not be completely filtered. The second peak near 404 nm is the Raman emission of water due to 355 nm excitation. The emission spectra of all samples are broad band emissions, indicating broad particle size distribution (Figure 7 and Table 1).[38] Peak widths are larger than those in the MAA-CdS system.[23]

Cd/S Ratio. The Cd/S ratio has been reported to be important for the size and properties of QDs coated with thiolated species.[23] Crystal sizes of 4.8, 3.7, and 3.9 nm were obtained at the Cd/S ratio of 0.6, 1.1, and 2.5, respectively, with PAA5K coating (Table 1). The major difference occurs when the S^{2-} amount exceeds Cd^{2+}. Surface passivization depends on the interaction of the carboxylates with the surface atoms. A strong adsorption of the coating on the crystal surface retards growth at that site. Carboxylates would not bind to anionic sulfur atoms on the crystal surface, eliminating an efficient surface capping and the desired arrested growth.

PL maximum is red-shifted by 110 nm, in agreement with larger crystal size, when the Cd/S ratio was reduced to 0.6 (Figure 7a). PL intensity was affected by the Cd/S ratio as well. At the compositions where Cd^{2+} is in excess (Cd/S = 1.1 and 2.5), PL intensities were comparable but showed a 3-fold decrease at the Cd/S ratio of 0.6. Similar results were also obtained for MAA stabilized CdS nanocrystals.[23] However, in that system there was about a 4-fold increase in PL intensity going from a Cd/S ratio of 1 to 2. Improved luminescence with the use of excess Cd^{2+} supports the discussion of an ineffective coating of sulfur-rich crystal surface with the negatively charged carboxylate groups, creating dangling bonds on the surface acting as surface traps. It has also been reported that S^{2-} vacancies can act as deep traps for photogenerated electrons in the conduction band, resulting in the red luminescence of CdS through transfer to surface molecules or to a preexisting trapped hole.[39]

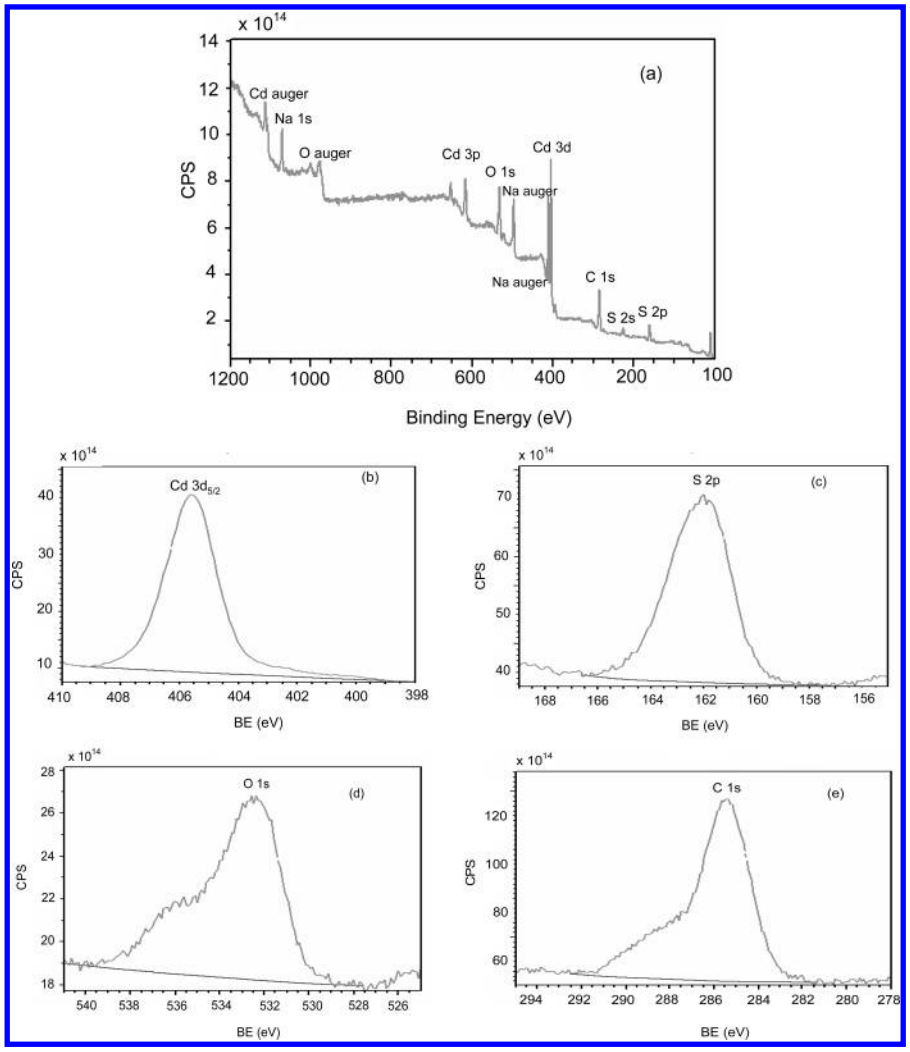

Figure 5. XPS spectra of (a) PAA 2K-2b: (b) Cd 3d, (c) S 2p, (d) O 1s, (e) C 1s.

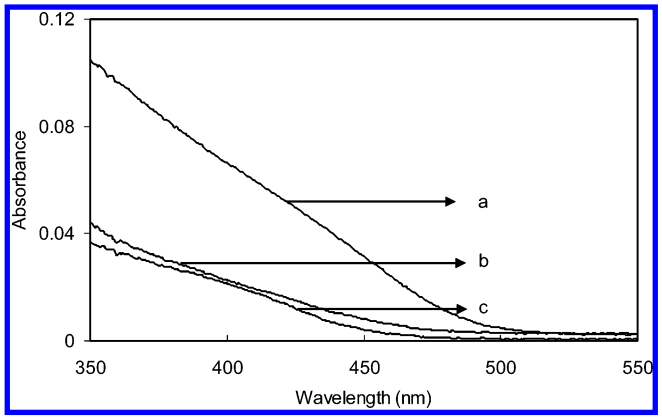

Figure 6. Absorption spectra of CdS NPs prepared at COOH/Cd = 1.6 using (a) PAA2K at pH = 5.5, (b) PAA5K at pH = 7.5, and (c) PAA2K at pH = 7.5.

Therefore, Cd/S ratio was fixed at 1.1 for the reactions designed to study the influence of polymer amount, polymer molecular weight, and reaction pH.

PAA Amount and Molecular Weight. The crystal size increases slightly with increasing amount of polymer (increasing COOH/Cd ratio from 1 to 12.5) at pH 7.5 (Figure 8) from 3.6 to 4.9 nm for PAA2K and from 3.7 to 6.5 nm for PAA5K (Table 1). It is important to note that crystal sizes are close to each other around a critical COOH/Cd ratio of 1.5−2 for both PAA molecular weights. Above this ratio, increasing the amount of polymer increases the crystal size at pH 7.5. Along with this, emission spectra showed maximum PL intensity around COOH/Cd = 1.5−2 as well (Figure 7). This should correspond to a ratio where a critical amount of surface cations are bound to the carboxylates, creating a relatively defect-free surface. Further increase in the coating amount causes a decrease in PL intensity. This is quite interesting since increasing the amount of surface capping agent is generally expected to decrease the crystal size and ensure full surface coverage, decreasing nonradiative coupling. However, PAA may behave differently than a monomeric carboxylate. The observed trend here points out ineffective or incomplete surface capping with increasing coating amount. A combination of factors such as particle bridging, extended polymer conformation, high charge density, and repulsion of the neighboring carboxylates that would adsorb on the particle surface could play a role in such a trend. These factors would be imposing more dramatic effects especially at higher COOH/Cd ratios and high molecular weights. Above the mentioned critical COOH/Cd ratio, PAA5K-coated NPs have larger crystal size (Figure 8) and lower PL intensity than PAA2K-coated ones (Figure 7b,d). Decreasing PL intensity with increasing coating amount have been reported with mercaptoacetic acid[23] and cystein[19] coated CdS QDs recently, but these systems contain thiols as the surface binding moiety, and the behavior, although not known exactly, was attributed to the competitive binding of Cd^{2+} to S^{2-} versus RS^{-} or the resulting change in pH. In our study, all reactions were performed at a

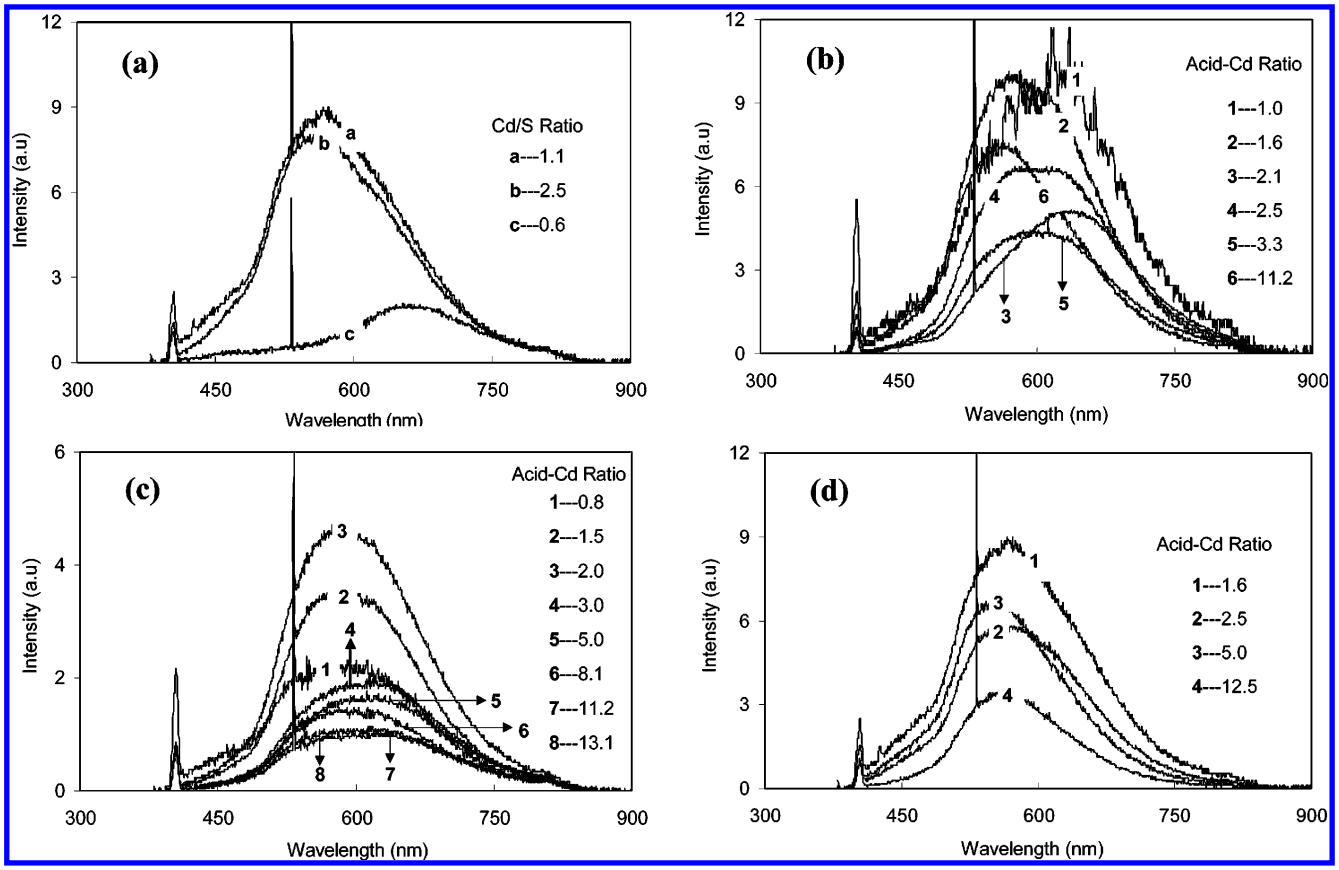

Figure 7. (a) Calibrated PL spectra of PAA5K-coated CdS with varying Cd/S ratio. Reaction pH = 7.5, and COOH/Cd = 1.6. (b) Calibrated PL spectra of PAA2K-coated CdS prepared at pH = 7.5. (c) Calibrated PL spectra of PAA2K-coated CdS prepared at pH = 5.5. (d) Calibrated PL spectra of PAA5K-coated CdS prepared at pH = 7.5.

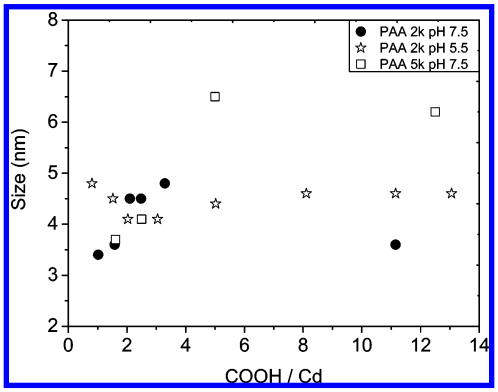

Figure 8. Variation of the crystal size as a function of COOH/Cd ratio for different values of PAA molecular weight and reaction pH.

fixed pH. Besides, affinity of Cd^{2+} to thiol is much higher than that to carboxylate. PAA forms complexes with the free Cd^{2+} in the solution and the particle surface during growth. Dynamic adsorption allows the crystal to grow through deposition of ions on the surface in a mechanism similar to ligand exchange and is known as cluster−cluster aggregation.[40] Since smallest crystal sizes are obtained at around a COOH/Cd ratio of 1.5−2, the best balance of surface and cation complexation should be achieved at this ratio. In his studies, Moffit focused on the synthesis of CdS in micelles of PAA/PS core/shell structures and emphasized the importance of kinetic control on particle size.[41] He suggests that the size of the CdS formed within micelles depends on the size of the ionic core and is limited by the viscosity that slows diffusion. In our case, there is no micelle but PAA-Cd^{2+} complexes might be considered as polymeric networks or clusters where many Cd^{2+} ions can form a complex with a single chain or where Cd^{2+} can form a complex with two different chains. Charge neutralization collapses the polymer to some extent, which would prefer rather extended conformation otherwise due to charge repulsion. Growth will be influenced by the diffusion rate of the ions and clusters in such a network, limiting the ability to tune particle size. This may also explain why blue or red luminescent particles could not be achieved with PAA in our work. At a fixed COOH/Cd ratio, a lesser amount of PAA5K is used in comparison to PAA2K, so the number of coating molecules decreases. As the size of the polymer chain increases, not only does the possibility of binding multiple Cd^{2+} increase but also the bridging between primary particles increases. This would increase the cluster−cluster collisions as well, enhancing growth. In addition, longer chains and the repulsion between the repeat units prevent effective passivization of the surface which allows growth through deposition of ions on the surface. Such a decrease in the surface passivization also leads into the observed drop in the luminescence of QDs with increasing COOH/Cd ratio and PAA molecular weight. Increasing the amount of coating does not help beyond the critical ratio since these charged macromolecules repel each other and prefer extended confirmation which is difficult for wrapping around the crystal surface. Negative influence of the chain length and increased charge density on the capping of the crystal surface and arresting crystal growth could explain the increasing size and decreasing luminescence. Incomplete surface capping/ passivization would leave uncoordinated sites as surface traps resulting in nonradiative recombination of the electron and the hole and hence reduced luminescence.

pH. CdS QDs were synthesized at pH 5.5 and 7.5. The initial complex formed between PAA and Cd^{2+} is insoluble below pH

4.0. In order to increase the binding capacity of PAA, a higher pH value of 7.5 was also adopted. Reaction pH has a significant influence on the crystal size and luminescence. Although overall variation in the crystal size as a function of COOH/Cd ratio is less dramatic at pH 5.5, as the ratio is increased from 0.5 to 2, size decreased from 4.8 to 4.1 nm and stayed around 4.7 nm above this ratio. This indicates the existence of a two-way interaction between the pH and the polymer amount in affecting the crystal size. At fixed COOH/Cd ratio, particles prepared at pH 5.5 absorb at longer wavelengths (Figure 6), suggesting less effective surface capping as a means to arrest the particle growth. At pH 5.5, luminescence intensities also dropped significantly (Figure 7b,c) and the PL maximum shifted to longer wavelengths in agreement with the absorbance spectra (Figure 6). Yang and Gao[21] reported pH-dependent luminescence for 3-mercaptopropionic acid (MPA) and thioglycolic acid (TGA)-coated CdTe, showing a maximum at pH 6 and 4.5, respectively. They have adjusted the pH during the measurements. They suggest that surface passivization is enhanced, though secondary interaction of the carbonyl of the protonated carboxylic acid group with the CdTe surface and the pH where protonation takes place depends on the pK_a of the acid. According to this hypothesis, PAA (pK_a = 4.75) should provide better luminescence at higher pH than MPA (pK_a = 4.32). More importantly, partial protonation of carboxylates at low pH results in a decrease in the electrostatic repulsion, collapses the polymer, and decreases the cation and surface binding ability. According to Rivas et al., PAA binds 50% more Cd^{2+} at pH 7.5 than at pH 5.5.[42] Parallel to this, surface binding ability of PAA would also decrease with the protonated acids since carboxylate is the effective surface binding group, resulting in larger crystal sizes and uncoordinated sites on the surface. One should consider that carboxylates are linked together on a polymer chain and electrostatic repulsion of the unprotonated carboxylates as well as H-bonding in the protonated acids would be influential in determining the adsorption of carboxylates in close proximity. After MPA addition to PAA-coated QDs, we have seen an increase in the fluorescence intensity of the particles qualitatively. This observation also points out that the bonding strength, coating chemistry, surface coverage, and the pK_a values of the surfactants are significant contributors to the fluorescence intensity. On the basis of the above discussion, for effective capture of surface cations with carboxylates, a higher amount of polymer might be needed at pH 5.5. This could explain the decreasing crystal size with increasing polymer amount at pH 5.5 as we approach the critical COOH/Cd ratio (Figure 8).

PL spectra showed a similar trend. pH also influences the optimum polymer amount required for the maximum luminescence intensity. At pH 5.5, PL intensity increases with increasing coating amount until the COOH/Cd ratio of 2 is reached and afterward it shows a downward trend as seen for both molecular weights at pH 7.5 and 5.5 (Figure 7b−d).

Quantum Yield. Comparison of the luminescence of QDs and the trend observed as a function of our variables can be clearly seen in the QYs calculated against a Rhodamine B reference. Figure 9 shows calculated relative QYs (η) for all samples. QY of CdS QDs is slightly better with PAA2K (8−17%) than with PAA5K at pH 7.5 (5−13%). Maximum QY obtained from CdS QDs prepared in a PS(300)-block-PAA(20) micelle was reported as 4%.[24] At similar sizes, we have obtained better QYs. In the reported example, a COOH/Cd ratio of 0.66 (Cd/COOH = 1.5) was used. At this ratio, insufficient surface coverage could diminish QY. We believe that in PAA-CdS QDs, at the ratios that we have studied, we achieved better surface passivization reducing the extent of nonradiative relaxations and improved the QY over the reported values.

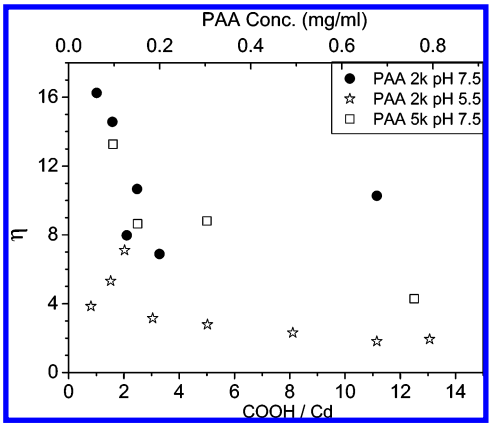

Figure 9. QY (η) of the samples as a function of reaction variables.

Overall, a significant decrease in the QY is observed at reaction pH 5.5. QY decreases with increasing coating amount at pH 7.5, but at pH 5.5, it has a bell-shaped trend with a maximum around COOH/Cd = 2, in agreement with PL intensity. CdS crystal size decreased as the COOH/Cd ratio increased to 2 as discussed in previous sections (Figure 8). It is important to note that this COOH/Cd ratio is the same critical ratio observed in UV analysis and corresponds to the smallest crystal sizes for the *stable* colloids in each series. Smaller crystal sizes may contribute to enhanced quantum efficiency as well. This further supports the importance and dependence of size and luminescence on the polymer amount−pH interaction.

No significant decrease in the QY of the particles was observed for over 8 months. The optimum COOH/Cd ratio for the best QY appears to be around the critical ratio of 1.5−2 for both molecular weights and pH without loosing colloidal stability.

Conclusions

CdS QDs were prepared successfully in a simple aqueous and relatively green route with a PAA coating of 2100 and 5000 g/mol molecular weight. An excellent long-term colloidal stability of the CdS QDs with functional surfaces was achieved, far beyond what we have observed with MAA systems. PAA-coated CdS NPs are luminescent mostly in the light yellow-orange with absorption in the range of 460−508 nm. Small size alterations between 3.6 and 6.5 nm can be achieved by increasing the amount (COOH/Cd in the range of 0.8−12.5) and molecular weight of PAA. However, significant size tuning accompanied with luminescence in a broader visible range cannot be achieved with this polyelectrolyte. PAA provides surface adsorbing groups that are dependent on each other. Repulsion of neighboring chains and COO^- groups would impact chain conformation, cause expansion, and impose restrictions in adsorption on the crystal surface and limitations in further size tuning. The complex formed between PAA and Cd^{2+} is influential on the size as well. Such complexes are formed by binding of multiple cations to a single PAA chain. Therefore, at a fixed COOH/Cd ratio, lower molecular weight polymers, providing more polymer chains, are more desirable. Carboxylates of PAA adsorb on the Cd^{2+}-rich surface much more effectively, and therefore, a Cd/S ratio above 1 is desirable for better surface capping, enabling better size control and better luminescence.

QYs of the PAA-coated CdS QDs are in the range of 5−17%. Data indicate that use of a large excess of PAA increases the

crystal size and decreases the PL intensity. A very important outcome of this study is the identification of an optimum COOH/Cd ratio around 1.5−2 for the highest PL intensity and QY for both molecular weights and pH (5.5 and 7.5) within the limits of colloidal stability. NPs prepared with the COOH/Cd ratio above 1 showed both colloidal and luminescence stability over 8 months so far. Reaction pH is also identified as a critical parameter for the QY and the particle size. NPs prepared at higher pH values where the polymer is mostly ionized provided better surface passivization and better QYs. For maximum QY and smaller crystal sizes, a larger amount of polymer is needed at lower pH where some protonation of the acid takes place. It is crucial to understand this critical ratio and the pH sensitivity for tuning particle size while keeping colloidal stability.

Here, we provided the first detailed study of PAA-coated CdS NPs. Although extremely stable and more luminescent than those reported by Moffit, PAA-coated CdS NPs do not have very high QY.[24] It is possible to improve the luminescence intensity and QY of these particles further by coating CdS crystals with ZnS or CdSe/ZnS as described in the literature.[43−45] The knowledge gained from this study can be applied to other polymers and QDs. CdS was used as a model QD here, especially because it emits in the visible range. We are currently investigating the methods to improve the properties of these QDs.

Acknowledgment. This work was partially financed by the Marie Curie Re-integration Grant (MIRG-CT-2006-031072). We thank Baris Yagci at Eindhoven University of Technology for the XPS analysis.

References and Notes

(1) Alivisatos, A. P. *J. Phys. Chem.* **1996**, *100*, 13226.
(2) Brus, L. E. *J. Chem. Phys.* **1984**, *80*, 4403.
(3) Schmid, G. *Nanoparticles: From Theory to Application*, 3rd ed.; Wiley-VCH: New York, 2005.
(4) Yu, W. W.; Qu, L. H.; Guo, W. Z.; Peng, X. G. *Chem. Mater.* **2004**, *16*, 560.
(5) Aldana, J.; Wang, Y. A.; Peng, X. G. *J. Am. Chem. Soc.* **2001**, *123*, 8844.
(6) Ozkan, M. *Drug Discovery Today* **2004**, *9*, 1065.
(7) Marti, A.; Lopez, N.; Antolin, E.; Canovas, E.; Stanley, C.; Farmer, C.; Cuadra, L.; Luque, A. *Thin Solid Films* **2006**, *511−512*, 638.
(8) Landi, B. J.; Castro, S. L.; Ruf, H. J.; Evans, C. M.; Bailey, S. G.; Raffaelle, R. P. *Solar Energy Mater. Solar Cells* **2005**, *87*, 733.
(9) Weng, J. F.; Song, X. T.; Li, L. A.; Qian, H. F.; Chen, K. Y.; Xu, X. M.; Cao, C. X.; Ren, J. C. *Talanta* **2006**, *70*, 397.
(10) Henini, M.; Bugajski, M. *Microelectron. J.* **2005**, *36*, 950.
(11) Mattheakis, L. C.; Dias, J. M.; Choi, Y. J.; Gong, J.; Bruchez, M. P.; Liu, J., E. W. *Anal. Biochem.* **2004**, *327*, 200.
(12) Yin, Y.; Alivisatos, A. P. *Nature* **2005**, *437*, 664.
(13) Spanhel, L.; Haase, M.; Weller, H.; Henglein, A. *J. Am. Chem. Soc.* **1987**, *109*, 5649.
(14) Murray, C. B.; Norris, D. J. *J. Am. Chem. Soc.* **1993**, *115*, 8706.
(15) Ji, J.; Rosenzweig, N.; Jones, I.; Rosenzweig, Z. *Anal. Chem.* **2001**, *73*, 3521.
(16) Luccardini, C.; Tribet, C.; Vial, F.; Marchi-Artzner, V.; Dahan, M. *Langmuir* **2006**, *22*, 2304.
(17) Fan, H. Y.; Leve, E. W.; Scullin, C.; Gabaldon, J.; Tallant, D.; Bunge, S.; Boyle, T.; Wilson, M. C.; Brinker, C. J. *Nano Lett.* **2005**, *5*, 645.
(18) Libert, S.; Gorshkov, V.; Privman, V.; Goia, D.; Matijevic, E. *Adv. Colloid Interface Sci.* **2003**, *100*, 169.
(19) Priyam, A.; Chatterjee, A.; Das, S. K.; Saha, A. *Res. Chem. Intermed.* **2005**, *31*, 691.
(20) Young, A. G.; Green, D. P.; McQuillan, A. J. *Langmuir* **2006**, *22*, 11106.
(21) Zhang, H.; Zhou, Z.; Yang, B.; Gao, M. Y. *J. Phys. Chem. B* **2003**, *107*, 8.
(22) Righini, G. C.; Verciani, A.; Pelli, S.; Guglielmi, M.; Martucci, A.; Fick, J.; Vitrant, G. *Pure Appl. Optics* **1996**, *5*, 655.
(23) Winter, J. O.; Gomez, N.; Gatzert, S.; Schmidt, C. E.; Korgel, B. A. *Colloids Surf., A* **2005**, *254*, 147.
(24) Wang, C. W.; Moffitt, M. G. *Langmuir* **2004**, *20*, 11784.
(25) Yusuf, H.; Kim, W. G.; Lee, D. H.; Guo, Y. Y.; Moffitt, M. G. *Langmuir* **2007**, *23*, 868.
(26) Duxin, N.; Liu, F. T.; Vali, H.; Eisenberg, A. *J. Am. Chem. Soc.* **2005**, *127*, 10063.
(27) Lu, X. F.; Gao, H.; Chen, J. Y.; Chao, D. M.; Zhang, W. J.; Wei, Y. *Nanotechnology* **2005**, *16*, 113.
(28) Raji, P.; Sanjeeviraja, C.; Ramachandran, K. *Cryst. Res. Technol.* **2004**, *39*, 617.
(29) Sondi, I.; Siiman, O.; Matijevic, E. *J. Colloid Interface Sci.* **2004**, *275*, 503.
(30) Chung, C. K.; Lee, M. *Bull. Korean Chem. Soc.* **2004**, *25*, 1461.
(31) Guinier, A. *X-ray Diffraction*; Freeman: San Francisco, 1963.
(32) Wang, W.; Liu, Z.; Zheng, C.; Xu, C.; Liu, Y.; Wang, G. *Mater. Lett.* **2003**, *57*, 2755.
(33) Whelan, C. M.; Ghijsen, J.; Pireaux, J.-J.; Maex, K. *Thin Solid Films* **2004**, *464/465*, 388.
(34) Farah, A. A.; Zheng, S. H.; Morin, S.; Bensebaa, F.; Pietro, W. J. *Surf. Sci.* **2007**, *601*, 1677.
(35) Kar, S.; Chaudhuri, S. *Synth. React. Inorg. Met.-Org. Nano-Met. Chem.* **2006**, *36*, 289.
(36) Chowdhury, P. S.; Ghosh, P.; Patra, A. *J. Lumin.* **2007**, *124*, 327.
(37) Wang, Y.; Suna, A.; Mahler, W.; Kasowki, R. *J. Chem. Phys.* **1987**, *87*, 7315.
(38) Wuister, S. F.; Meijerink, A. *J. Lumin.* **2003**, *102*, 338.
(39) Trindade, T.; OBrien, P.; Zhang, X. M. *Chem. Mater.* **1997**, *9*, 523.
(40) Swayambunathan, V.; Hayes, D.; Schmidt, K. H.; Liao, Y. X.; Meisel, D. *J. Am. Chem. Soc.* **1990**, *112*, 3831.
(41) Moffitt, M.; McMahon, L.; Pessel, V.; Eisenberg, A. *Chem. Mater.* **1995**, *7*, 1185.
(42) Rivas, B. L.; Pereira, E. D.; Moreno-Villoslada, I. *Prog. Polym. Sci.* **2003**, *28*, 173.
(43) Reiss, P.; Carayon, S.; Bleuse, J.; Pron, A. *Synth. Met.* **2003**, *139*, 649.
(44) Hines, M. A.; Guyot-Sionnest, P. *J. Phys. Chem.* **1996**, *100*, 468.
(45) Gerion, D.; Pinaud, F.; Williams, S. C.; Parak, W. J.; Zanchet, D.; Weiss, S.; Alivisatos, A. P. *J. Phys. Chem. B* **2001**, *105*, 8861.